

See discussions, stats, and author profiles for this publication at: <https://www.researchgate.net/publication/322901001>

A class of electrically small spherical antennas with near-minimum Q

Conference Paper · September 2008

CITATION

1

READS

462

2 authors:



Jacob Adams

North Carolina State University

85 PUBLICATIONS 3,000 CITATIONS

SEE PROFILE



J.T. Bernhard

University of Illinois, Urbana-Champaign

175 PUBLICATIONS 5,865 CITATIONS

SEE PROFILE

A CLASS OF ELECTRICALLY SMALL SPHERICAL ANTENNAS WITH NEAR-MINIMUM Q

Jacob J. Adams and Jennifer T. Bernhard
Electromagnetics Laboratory
University of Illinois at Urbana-Champaign, Urbana, IL 61801
<http://antennas.ece.uiuc.edu>; E-mail: jbernar@uiuc.edu

Abstract: We theoretically describe and experimentally demonstrate a new class of electrically small spherical antennas with near minimum radiation Q . The antenna operates by exciting the TM_{10} spherical mode and minimizing excitation of higher order modes. The antenna compares favorably to existing electrically small antennas and can be easily designed for any frequency or with any electrical size. Methods for matching the antenna as well as measured results are presented.

1. Fundamental Limitations of Electrically Small Antennas

One of the key parameters for electrically small antennas is the radiation quality factor (Q). The Q of an antenna represents the ratio of the energy stored per cycle to the power radiated and is typically defined as

$$Q_{rad} = \frac{2\omega_0 |W_{max}|}{P} \quad (1)$$

Radiation Q is critical for a singly resonant antenna, because the antenna's bandwidth is inversely proportional to Q [1]. Thus, a low Q antenna is desirable.

However, Q has been shown to be constrained by the electrical size of the antenna. In 1948, Chu published his well-known work investigating the fundamental limitations of antennas [2]. He showed that the radiation Q of an antenna has a lower limit determined by the electrical size of a sphere of radius a which circumscribes the antenna [2], [3].

$$Q_{Chu} \approx \frac{1}{ka} + \frac{1}{(ka)^3} \quad (2)$$

We will refer to this as the Chu limit. An antenna that approaches Chu's limit has been sought after for decades. It has been taken as a rule of thumb that an antenna that most fully occupies a spherical volume exhibits the lowest Q . Foltz and McLean showed mathematically that the minimum Q is achievable with an antenna occupying a spherical volume rather than a dipole or planar structure [4]. In agreement with these principles,

Best introduced a spherical wire antenna with among the lowest Q to date at approximately $1.5 \times Q_{Chu}$ [5], [6]. However in [6], the antenna was found to be tunable to 50Ω only for certain electrical sizes. In this paper, we describe a spherical antenna that offers similar Q performance to the spherical helix and the added advantage of tunability. Our design approach is unusual in that a low Q current distribution is described mathematically and the structure of the antenna is manipulated to achieve it.

2. A TM_{10} Antenna

In our discussion of Q , it should be noted that Chu's limit may be overly optimistic. As observed by Chu himself, the model does not consider energy stored within the circumscribing sphere. This energy would increase the Q , so the actual bound must be higher than Chu calculated. Thal recently addressed this shortcoming by deriving a modal circuit model which also includes internal stored energy [7]. The new model results in a higher limit on the minimum Q .

To simplify the mathematics, Thal considered only currents on a spherical surface. In his model, the lowest possible Q for currents on a spherical surface is obtained by exciting the TM_{10} spherical mode while minimizing excitation of higher order modes which primarily store energy. The TM_{10} mode can be excited by a surface current distribution of the form [7]

$$J_\theta = \sin(\theta) \quad (3)$$

The primary challenge is engineering such a current distribution. An antenna structure supporting this distribution was introduced in [8]. In order to approximate the desired distribution, several wires are placed along the constant- φ lines of a sphere. The sphere is bisected by a ground plane along $\theta = \pi/2$. In this configuration, the φ -directed wires are electrically short and produce a current distribution that is triangular in θ . To achieve the required full sinusoidal variation described above, the electrical length of the wires is increased by winding them in a helical fashion about the constant- φ lines.

A symmetric feed structure is required in order to provide equal excitation to the arms. A conducting trace suspended above the ground plane contacts all of the arms at their base. The trace is fed in the center by a probe from behind the ground plane. Figure 1 shows the proposed structure using four arms.

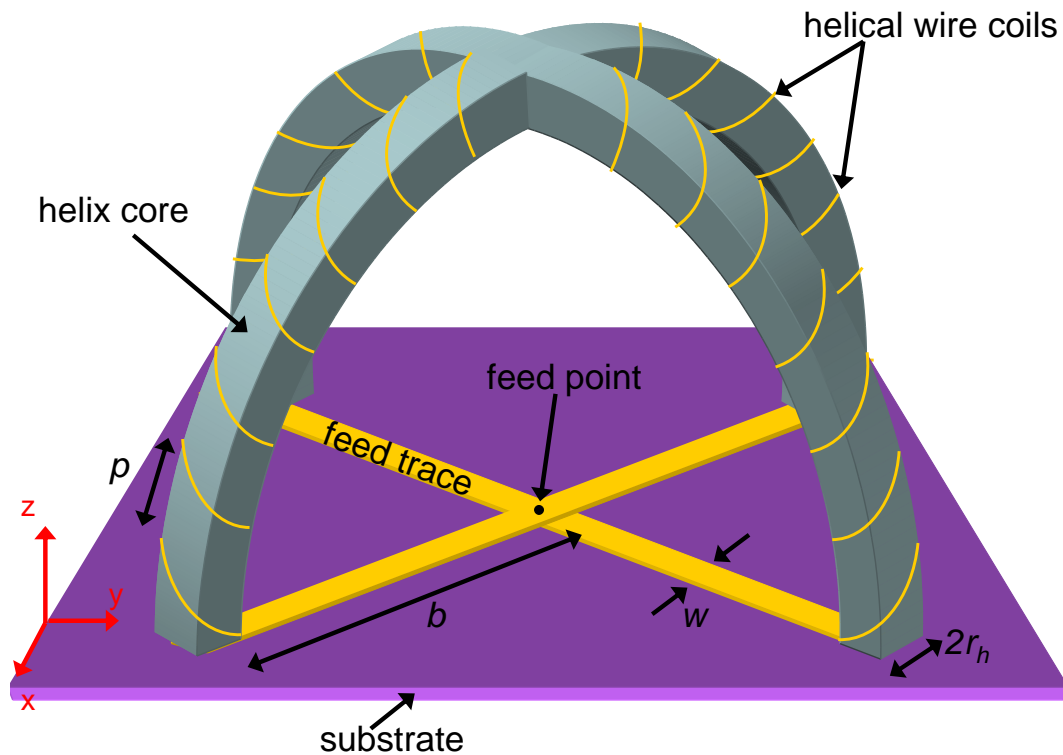


Figure 1: A four arm TM_{10} antenna. The pitch, p , is measured on the outer radius of the arm coils. The arm coils have radius r_h and their centerline follows a circle of radius b from the center of the structure. The width of the trace is w_t .

3. Properties of the Antenna

The antenna described in the previous section was simulated in using Ansoft's HFSS. In the electrically small region, the antenna exhibits some notable properties. A typical plot of the input impedance of the antenna is shown in Figure 2a. The first resonance of the antenna occurs when the physical length of wire on each arm is on the order of a half wavelength. Thus the pitch of the coils acts as the primary tuning mechanism by changing the electrical length of the arms. Decreasing the pitch lowers the resonant frequency. An antiresonance also appears in the electrically small region, slightly higher in frequency than the resonance.

When placed on an infinite ground plane, the antenna exhibits an electric monopole radiation pattern typical of most electrically small antennas. It is nearly omnidirectional in ϕ (variation of less than 0.4 dB for the four arm design), and it features a null at $\theta = 0$ and peak directivity of 9.4 dB along the direction of the ground plane ($\theta = 90^\circ$). The maximum cross polarization ratio is less than -40 dB.

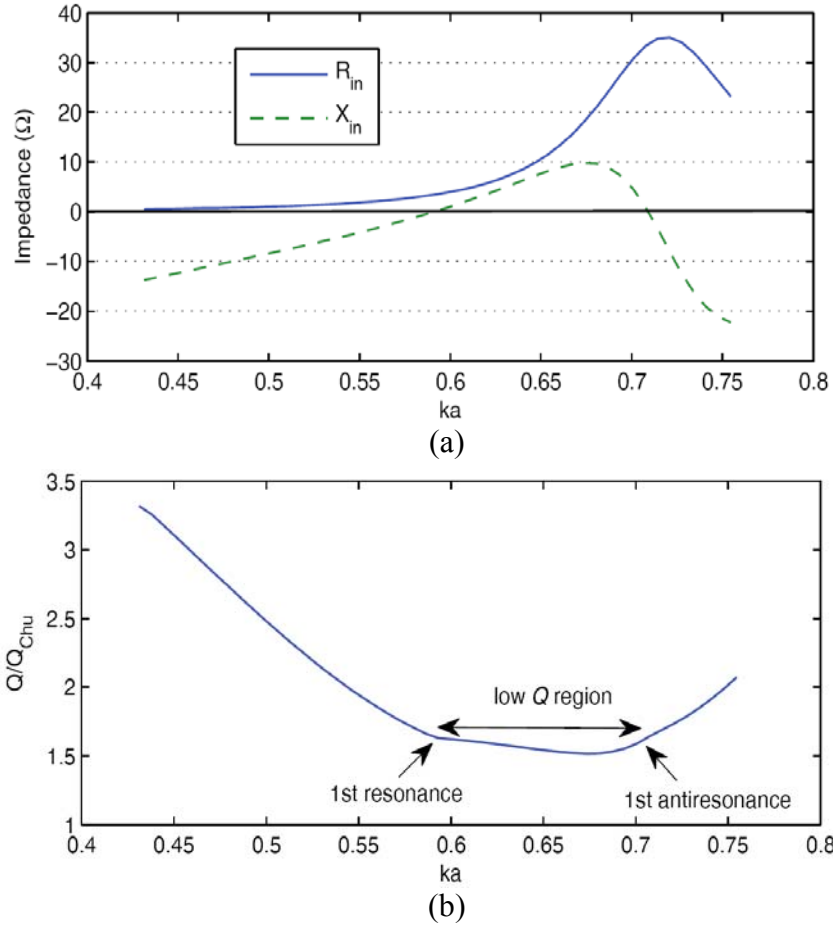


Figure 2: Typical properties of the TM_{10} antenna. (a) shows the input impedance behavior of the antenna in the electrically small region. (b) shows the Q/Q_{Chu} for the same antenna. The operating region or “low Q region” exists between the first resonance and the first antiresonance.

3.1 Behavior of the Quality Factor

The antenna’s bandwidth performance will be discussed in terms of the ratio Q/Q_{Chu} . This figure of merit clearly compares the TM_{10} antenna’s performance to the optimum, and performance can be fairly compared across different ka values. In all Q calculations, the input impedance is used to find Q using [1]

$$Q(\omega_0) = \frac{\omega_0}{2R(\omega_0)} \sqrt{\left[\frac{\partial}{\partial \omega} R(\omega_0) \right]^2 + \left[\frac{\partial}{\partial \omega} X(\omega_0) + \frac{|X(\omega_0)|}{\omega_0} \right]^2} \quad (4)$$

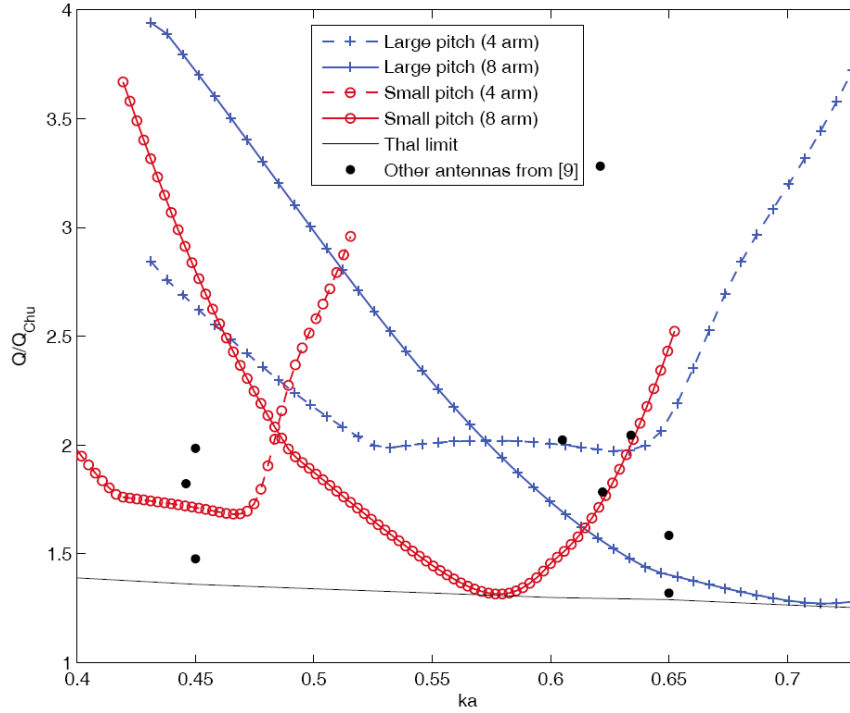


Figure 3: Q/Q_{Chu} ratio of several TM_{10} antennas compared to existing designs from [9]. The Thal limit for currents on a spherical surface [7] is also shown.

Figure 2b shows the Q/Q_{Chu} ratio for the same antenna whose impedance characteristics are shown. After the first resonance, the steep Q/Q_{Chu} curve flattens and reaches a minimum value. Then just before the subsequent antiresonance, the Q/Q_{Chu} value begins rising again. We refer to this flat region where the Q/Q_{Chu} minimum occurs as the “low Q region” indicating that the Q is low relative to the electrical size. Operation anywhere in this region is desirable.

3.2 Comparison to lower bound

The purpose of this study is to maximize performance (as measured by Q) with a realizable electrically small antenna. As discussed earlier, Thal has shown that the real achievable Q is higher than Chu’s limit when the currents are constrained to a spherical surface. Still, we will use the Chu limit as a basis for comparison but also present Thal’s limit for a more realistic assessment of antenna performance.

Illustrating the excellent performance of our design, Figure 3 shows the Q/Q_{Chu} ratio for the TM_{10} antenna with 4 arms and 8 arms and with two different pitches. Also shown in the plot are the Thal limit and several other designs from [9], the spherical helix, spherical cap monopole, and top loaded dipole. With 8 arms, the TM_{10} antenna closely

approaches the Thal limit, achieving nearly optimal Q and maximizing bandwidth. In addition to approaching the lower bound, the antenna exhibits Q lower than or equal to that of the comparison designs.

Finally, it can also be seen in Figure 3 that the operating frequency of the TM_{10} antenna can be moved by increasing and decreasing the pitch of the wires. The small pitch and large pitch designs shown here are given only as examples. An even smaller or larger pitch could be used to tune the operating frequency lower or higher, respectively.

4. Impedance Matching

Even if the antenna is operating in the low Q region, it still must be matched to the system impedance to achieve maximum bandwidth (the Q discussed in this work represents the Q when matched). As seen in Figure 2, the resistance at resonance is very small ($\sim 4\Omega$) and changes little when the geometric parameters are changed. However, at the antiresonance, the resistance can be varied greatly.

The primary factor in determining the antiresonant resistance (R_{ar}) is the electrical size of the structure. Figure 4 shows how R_{ar} varies as the antenna is tuned via pitch changes for a four arm antenna. The total size of the structure stays constant but the resonant frequency changes, so ka at antiresonance changes. When the antenna is tuned for very small electrical sizes, R_{ar} becomes very large.

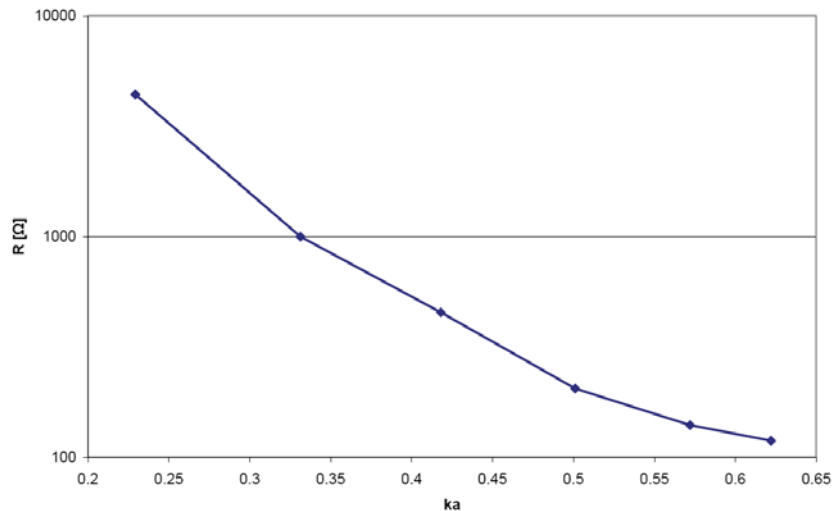


Figure 4: Antiresonant resistance (R_{ar}) versus electrical size (at antiresonance) of a four arm TM_{10} antenna with a .050" substrate ($\epsilon_r = 1$) and a trace width of 2 mm. As the antenna is tuned to smaller electrical sizes by lengthening the wire and changing the pitch, R_{ar} increases rapidly.

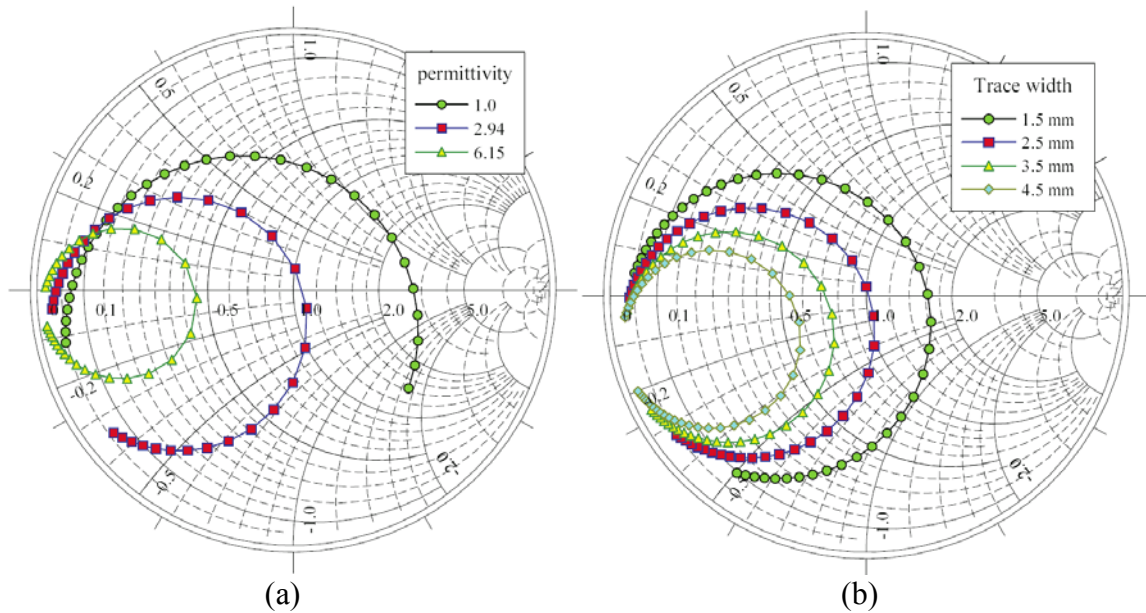


Figure 5: (a) Impedance of a four arm TM_{10} antenna ($ka = .47 - .62$) on a $.050''$ substrate with varying permittivity. Increasing the permittivity decreases R_{ar} . Trace width is 2 mm, $p = 3$ mm, $b = 21$ mm, $r_h = 2.5$ mm. (b) Impedance of a four arm TM_{10} antenna ($ka = .47 - .60$) with a $.050''$ substrate ($\epsilon_r = 2.94$). Decreasing the trace width increases R_{ar} . Other dimensions are: $p = 2.85$ mm, $b = 21$ mm, $r_h = 2.5$ mm.

4.1 Tuning via Parallel Capacitance

The parallel capacitance between the feed trace and the ground can also be adjusted to change R_{ar} . As the capacitance is decreased, R_{ar} increases. Shunt capacitance could be added with lumped capacitors, but they would incur losses and add complexity. Considering the configuration of the TM_{10} antenna, a significant source of parallel capacitance is already present between the feed trace and the ground plane. This capacitance can be adjusted by changing the substrate permittivity or the feed trace width.

As the dielectric constant of the substrate is increased, so is the capacitance. Figure 5a shows the impedance of the antenna for three different substrates. As ϵ_r increases, R_{ar} at for all ka values decreases. The impedance loop closes noticeably as the permittivity is decreased and the antiresonant frequency will be shifted lower. Other than the frequency shift, the Q/Q_{Chu} ratio is not significantly affected by the changing permittivity.

The substrate permittivity provides a coarse tuning option while the width of the feed trace allows finer control of the impedance. Figure 5b shows the effect of changing the trace width. The increased capacitance of a wider feed line decreases R_{ar} , as expected. The impedance change achieved with the trace width is much finer than what can be

achieved with the substrate permittivity. The change in antiresonant frequency is also smaller.

5. Measurements

A four arm version of the antenna was constructed and is shown in Figure 6. The antenna was tuned so that it was near 50Ω at 1.03 GHz ($ka = .52$). The feed trace was laid out on a .050" Duroid 6002 ($\epsilon_r = 2.94$) board which was 30.7 x 23.1 cm (1.06 x .801 λ_0). It should be noted that at sizes below 1.25λ , the ground plane no longer acts as an infinite ground and can affect the impedance, Q , and radiation pattern of the antenna.

The other dimensions (refer to Figure 1) were: $b = 21$ mm, $r_h = 2.5$ mm, $p = 2.85$ mm, $w = 2.5$ mm. The arms were constructed using a plastic ring ($\epsilon_r \approx 4$) as the core around which the wire was wrapped. The entire antenna, from the ground plane to the outer radius of the helix, fits into a sphere of radius 24 mm.

Simulated and measured input impedance of the antenna are shown in Figure 7. The measured half power bandwidth is 9.5% and the 2:1 VSWR bandwidth is 3.4%. The measured bandwidths result in a Q of 21.1 (computed using half power bandwidth) or 20.8 (computed using 2:1 VSWR bandwidth) [1]. The Chu limit for at this electrical size is 8.9, so the constructed antenna has Q of slightly around $2.35 \times$ the Chu limit. The tested design had four arms, but if more arms are added, the Q can more closely approach the limit.

The simulated Q at the operation point was 19.4, so the measured antenna has slightly smaller bandwidth than expected. This can be attributed to imperfections in the antenna's construction. In particular, the antenna's arms are not coiled perfectly and are slightly out of line with each other. Antenna efficiency was measured to be 89% using a Wheeler cap [10] while simulations showed 92% efficiency.

The finite ground plane causes the ideal current distribution given in equation 3 to be disrupted as image theory is no longer applicable. The radiation pattern and the Q differ noticeably from those of the antenna on an infinite ground. As seen in Figure 8, a sizeable lobe of back radiation appears, and the angle of maximum radiation is shifted from $\theta = 90^\circ$ to $\theta = 43^\circ$. In the azimuthal pattern, the co-polar component remains nearly omnidirectional with a maximum variation of 1.3 dB. However, the cross-polarization is significant in this plane, and at a few angles it is larger than the co-polarization.



Figure 6: A photograph of the constructed antenna.

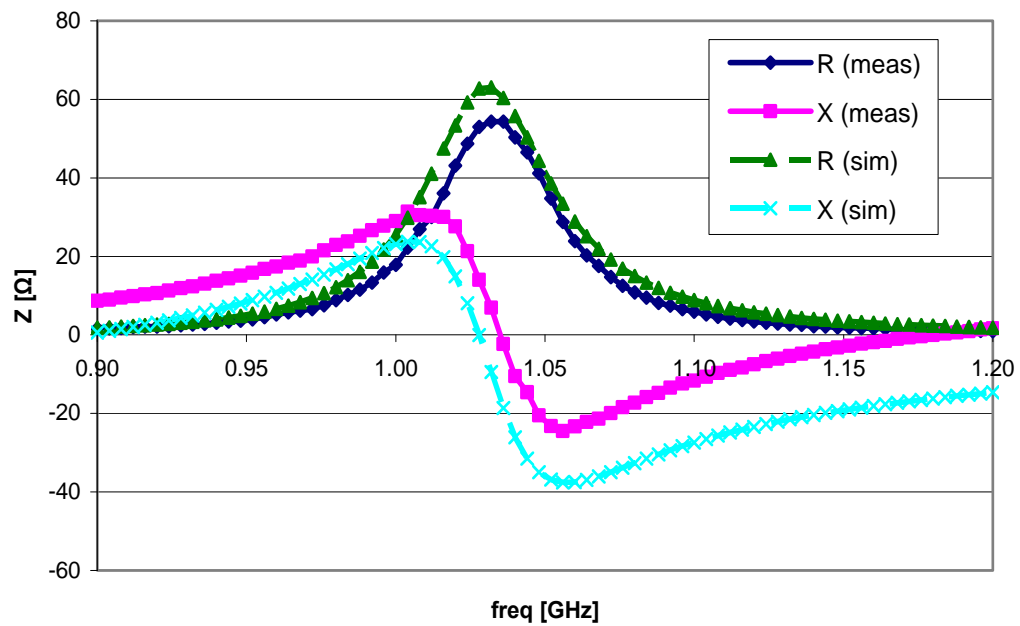


Figure 7: Simulated and measured input impedance of TM_{10} antenna ($ka = 0.48$).

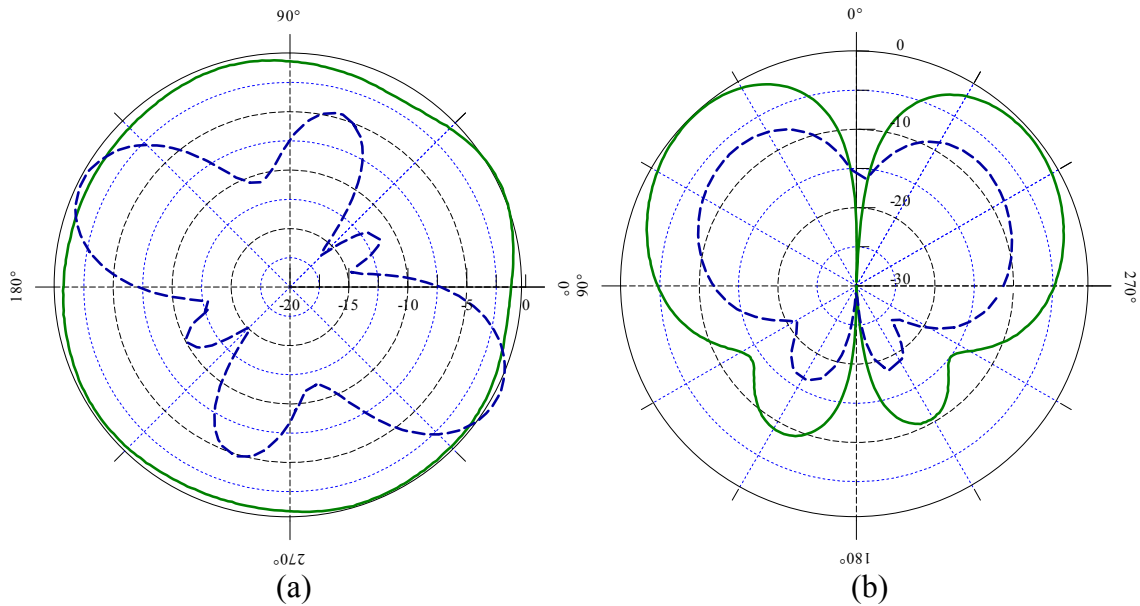


Figure 8: Normalized radiation patterns of the constructed antenna at 1.04 GHz. The co-polar component is shown with a solid line and cross-polar with a dotted line. Patterns were taken along (a) $\theta = 0$ and (b) $\phi = 0$.

6. Conclusion

We have introduced a new class of electrically small antennas operating in the TM_{10} mode to minimize Q . These antennas exhibit excellent Q performance, approaching the lower bound derived by Thal [7] as the number of arms is increased. They also exhibit Q comparable to some of the best existing designs from [9]. As an added advantage, they can be tuned to operate in the TM_{10} mode at any frequency and for any electrical size in the electrically small region via changes in coil pitch. They can also be matched to 50Ω without an external matching network using several tuning mechanisms introduced in this work.

A prototype antenna has been constructed and matched well to the simulated results. In future work, further measurements will be performed to investigate the behavior of the antenna at different electrical sizes. The impedance changes due to self capacitance will also be explored and a circuit model of the antenna will be developed. Finally, ground plane effects on the Q and radiation pattern of the antenna will be further studied.

Acknowledgments

This work is supported under a National Science Foundation Graduate Research Fellowship. The dielectric substrate materials for this work were provided by Rogers Corp.

References

- [1] A. D. Yaghjian and S. R. Best, "Impedance, bandwidth, and Q of antennas," *IEEE Trans. Antennas Propag.*, vol. 53, no. 4, pp. 1298–1324, April 2005.
- [2] L. J. Chu, "Physical limitations of omni-directional antennas," *J. Appl. Phys.*, vol. 19, no. 12, pp. 1163–1175, Dec. 1948.
- [3] J. S. McLean, "A re-examination of the fundamental limits on the radiation Q of electrically small antennas," *IEEE Trans. Antennas Propag.*, vol. 44, no. 5, pp. 672–676, May 1996.
- [4] H. D. Foltz and J. S. McLean, "Limits on the radiation Q of electrically small antennas restricted to oblong bounding regions," in *Proc. 1999 IEEE Antennas and Propagation Int. Symp.*, pp. 2702–2705.
- [5] S. R. Best, "The radiation properties of electrically small folded spherical helix antennas," *IEEE Trans. Antennas Propag.*, vol. 52, no. 4, pp. 953–960, April 2004.
- [6] S. R. Best, "Low Q electrically small linear and elliptically polarized spherical dipole antennas," *IEEE Trans. Antennas Propag.*, vol. 53, no. 3, pp. 1047–1053, March 2005.
- [7] H. L. Thal, "New radiation Q limits for spherical wire antennas," *IEEE Trans. Antennas Propag.*, vol. 54, no. 10, pp. 2757–2763, Oct. 2006.
- [8] J. J. Adams and J. T. Bernhard, "A low Q electrically small spherical antenna," in *Proc. 2008 Antennas and Propagation Int. Symp.*, 2008.
- [9] S. R. Best, "A study of the performance properties of small antennas," in *Proc. 2007 Antenna Appl. Symp.*, pp. 193–219.
- [10] W. E. McKinzie, "A modified Wheeler cap method for measuring antenna efficiency," in *Proc. 1997 IEEE Antennas and Propagation Int. Symp.*, pp. 542–545.